# SUPPLEMENTARY INFORMATION

# *In Vivo* Evolution of an Emerging Zoonotic Bacterial Pathogen in an Immunocompromised Human Host

Launay A[1], Wu CJ[1], Dulanto Chiang A[1], Youn JH[2], Khil PP[1,2], Dekker JP[1,2#]

[1]Bacterial Pathogenesis and Antimicrobial Resistance Unit, LCIM, NIAID, Bethesda, MD; [2]Dept. Laboratory Medicine, NIH Clinical Center, Bethesda, MD

#Address correspondence to John Dekker at john.dekker@nih.gov

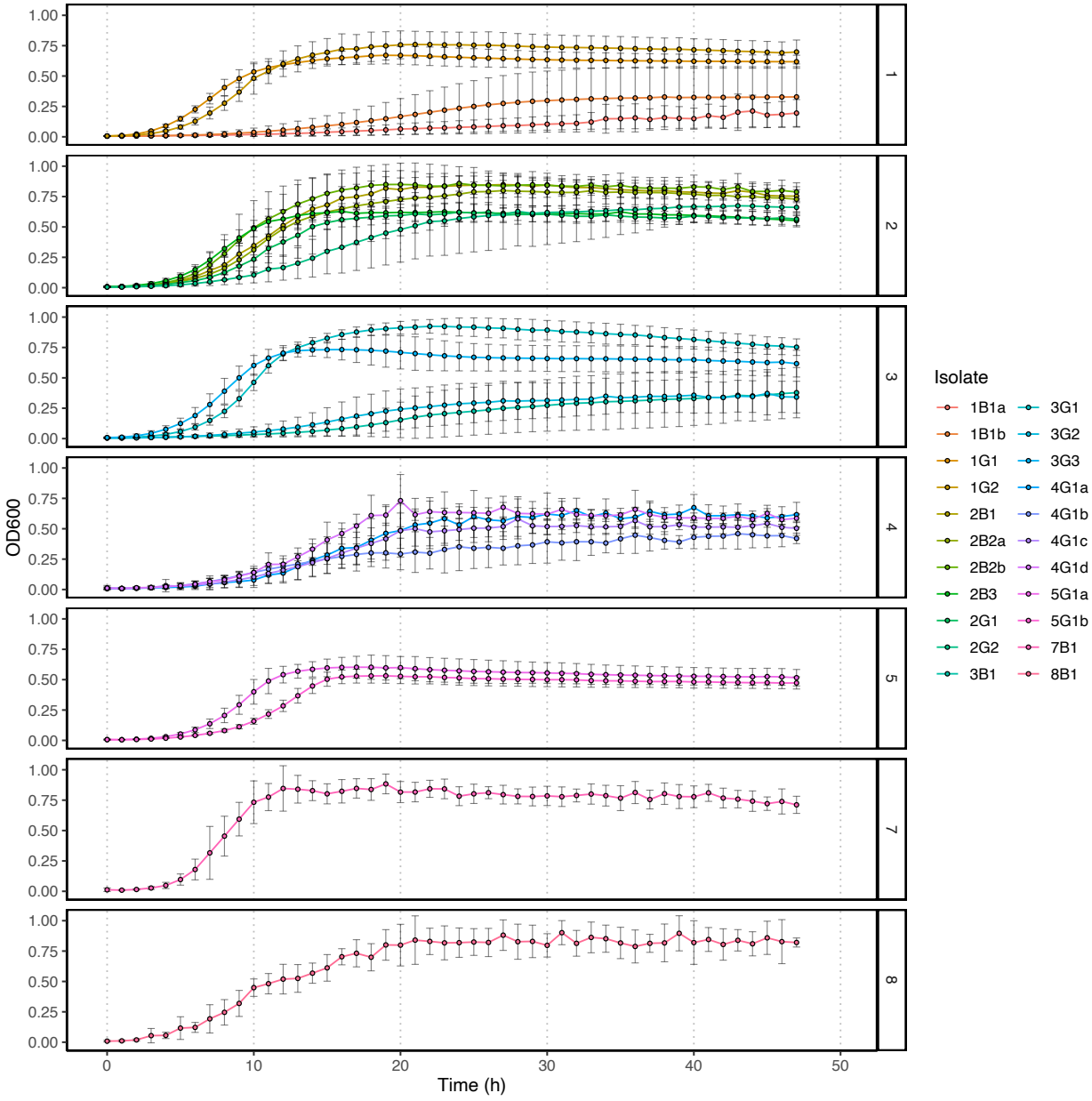


**Supplementary Figure 1. Growth curves of patient *B. hinzii* isolates show significant variability.** Growth in rich media at 37°C as measured by optical density at 600 nm. Points represent mean OD 600 value of replicates plotted on a linear scale, and the error bars indicate the standard deviation. Isolates are grouped by original date of isolation represented as culture number. Culture number 1: 1B1a (n = 7), 1B1b (n = 6), 1G1 (n = 3), 1G2 (n = 5); Culture number 2: 2B1 (n = 7), 2B2a (n = 7), 2B2b (n = 5), 2B3 (n = 6), 2G1 (n = 7), 2G2 (n = 6); Culture number 3: 3B1 (n = 7), 3G1 (n = 6), 3G2 (n = 7), 3G3 (n = 7); Culture number 4: 4G1a (n = 7), 4G1b (n = 7), 4G1c (n = 7), 4G1d (n = 7); Culture number 5: 5G1a (n = 5), 5G1b (N = 5); Culture number 7: 7B1 (N = 7); Culture number 8: 8B1 (N = 7). Isolate identities are given in legend at right. Note the extreme degree of variability in time to reach stationary phase, ranging from ~10 hr (7B1) to >25 hr (1B1a and 1B1b).

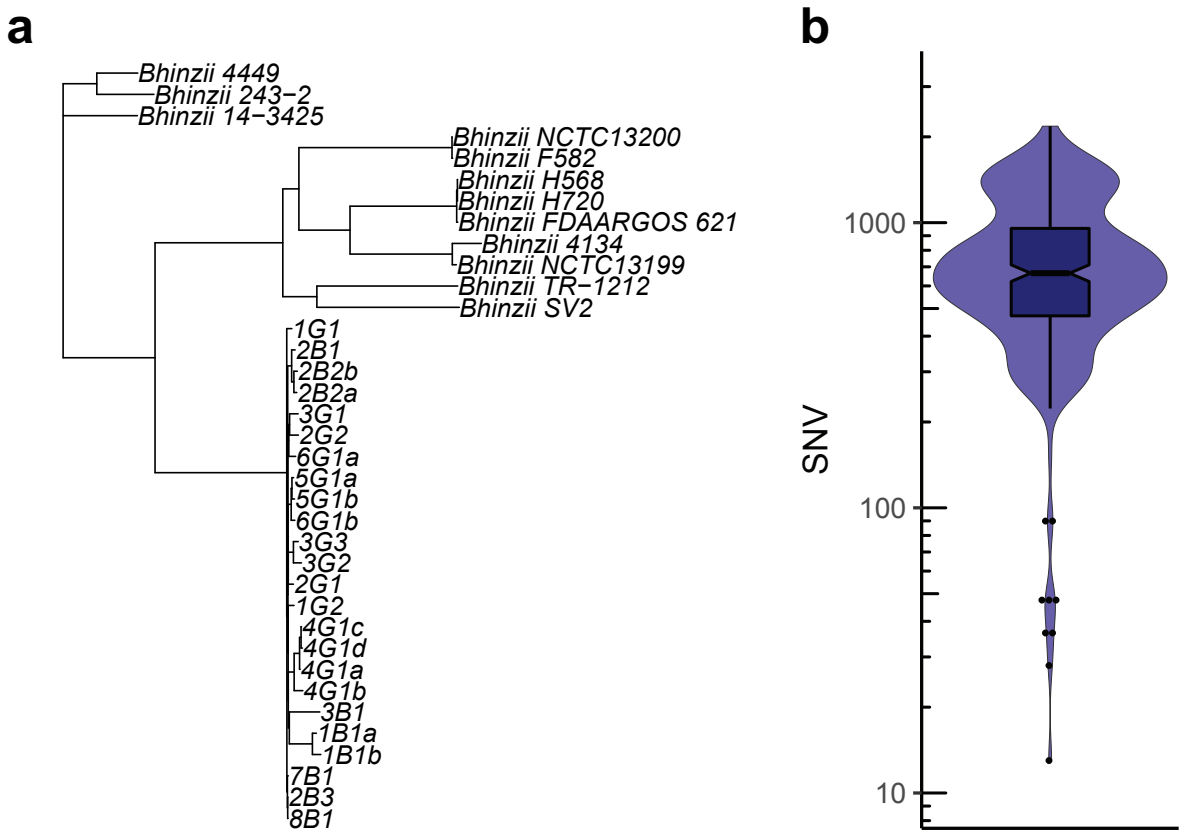


**Supplementary Figure 2. *B. hinzii* isolates cultured from patient form a single lineage with a striking range of divergence. a,** Core genome phylogeny generated with RAxML using the GTRGAMMA model, constructed from patient isolates in this study and publicly available *B. hinzii* genomes (downloaded from NCBI). The patient isolates are seen to form a distinct clade. **b**, Violin plot demonstrating pairwise divergence values for patient *B. hinzii* isolates (number of comparisons N = 276). Horizontal lines inside boxes indicate median values, the upper and lower edges correspond to the 25th and 75th percentiles, and whiskers extend to 1.5 × IQR. Outlier values outside of 1.5 × IQR represented as dots. A large range of pairwise divergence values is observed.

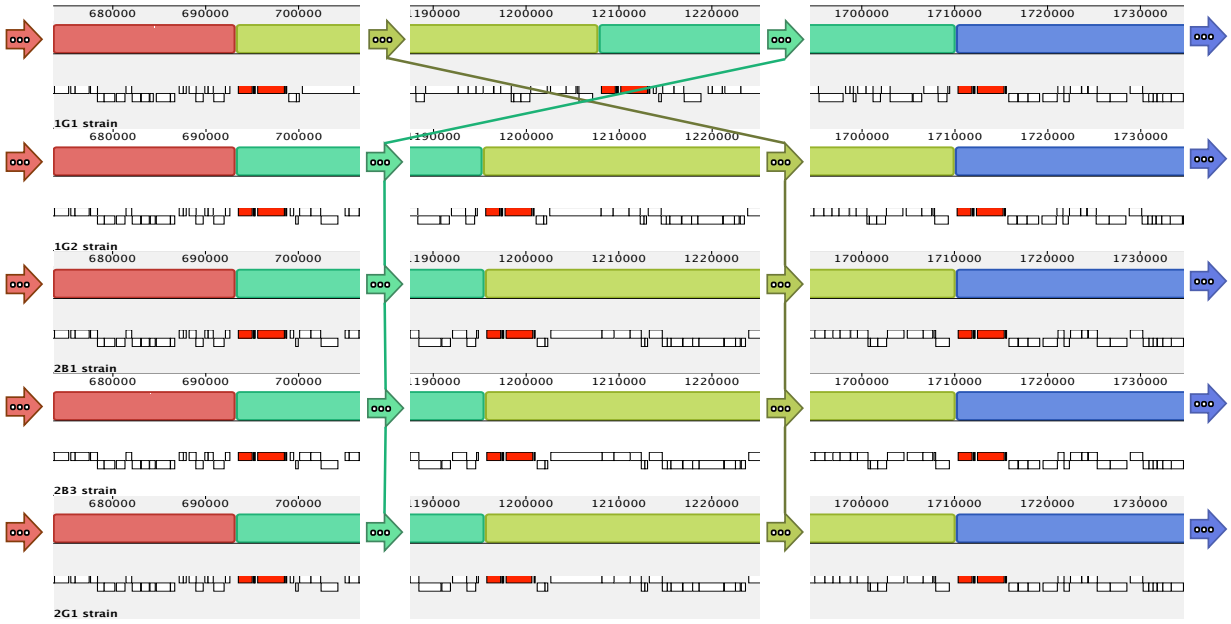


**Supplementary Figure 3. The genome of isolate 1G1 contains a 500 Kb translocation and a 53 Kb deletion.** Comparison (from top to bottom) of a region of genome from isolates 1G1, 1G2, 2B1, 2B3, and 2G1. A 500kb translocation is visible in 1G1. The translocated segment is flanked by rRNA sequences, highlighted in red in the annotation below each genome segment, suggesting a potential mechanism of recombination.

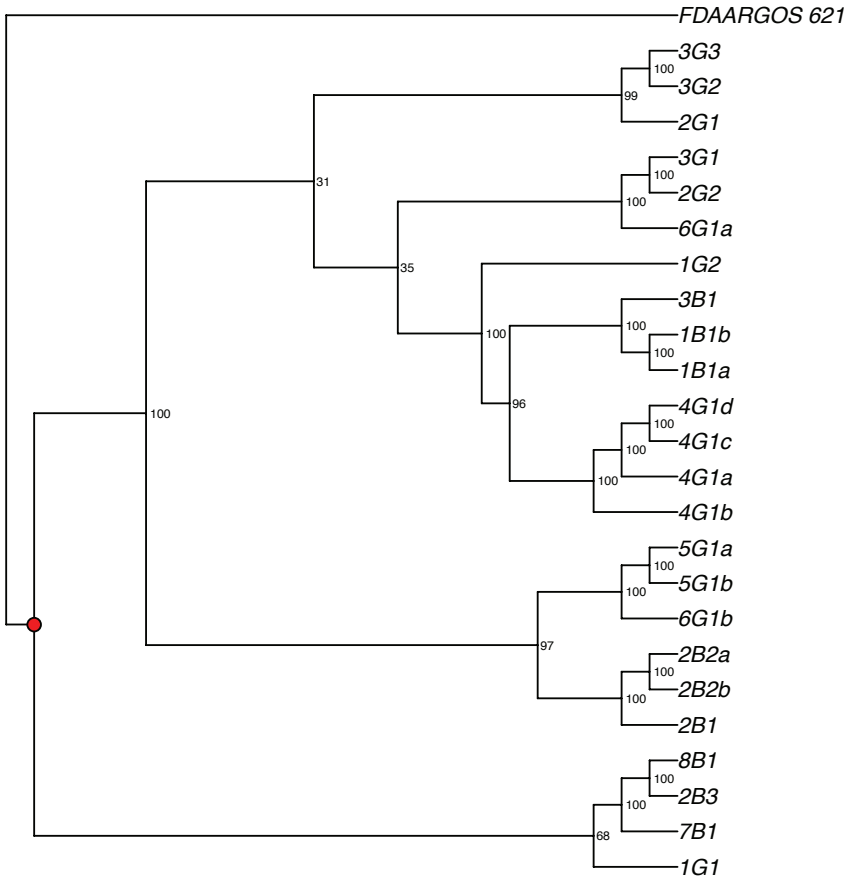


**Supplementary Figure 4. Rooted cladogram of patient isolates.** ML core genome phylogeny of patient isolates and FDA_Argos 621 as *B. hinzii* outgroup generated with RAxML using the GTRGAMMA model. The lowest common ancestor (LCA) of the patient clade is indicated with the red dot. The numbers at the node of the tree indicate bootstrap support.

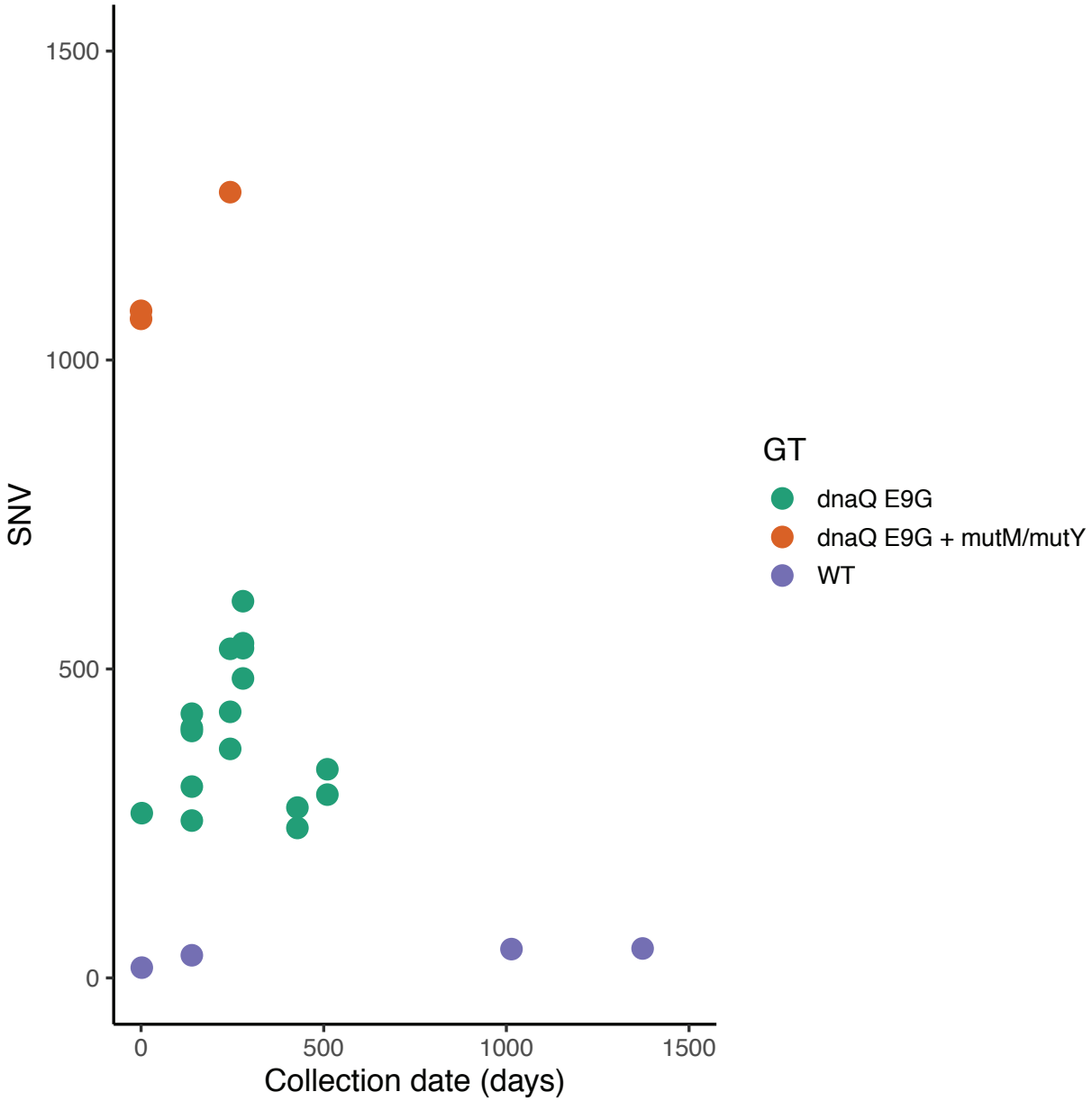


**Supplementary Figure 5. Divergence of patient isolates from LCA versus collection date.** The number of SNVs present in different patient isolates collected on different days is plotted. Genotype class is distinguished by color as indicated in the legend at right.

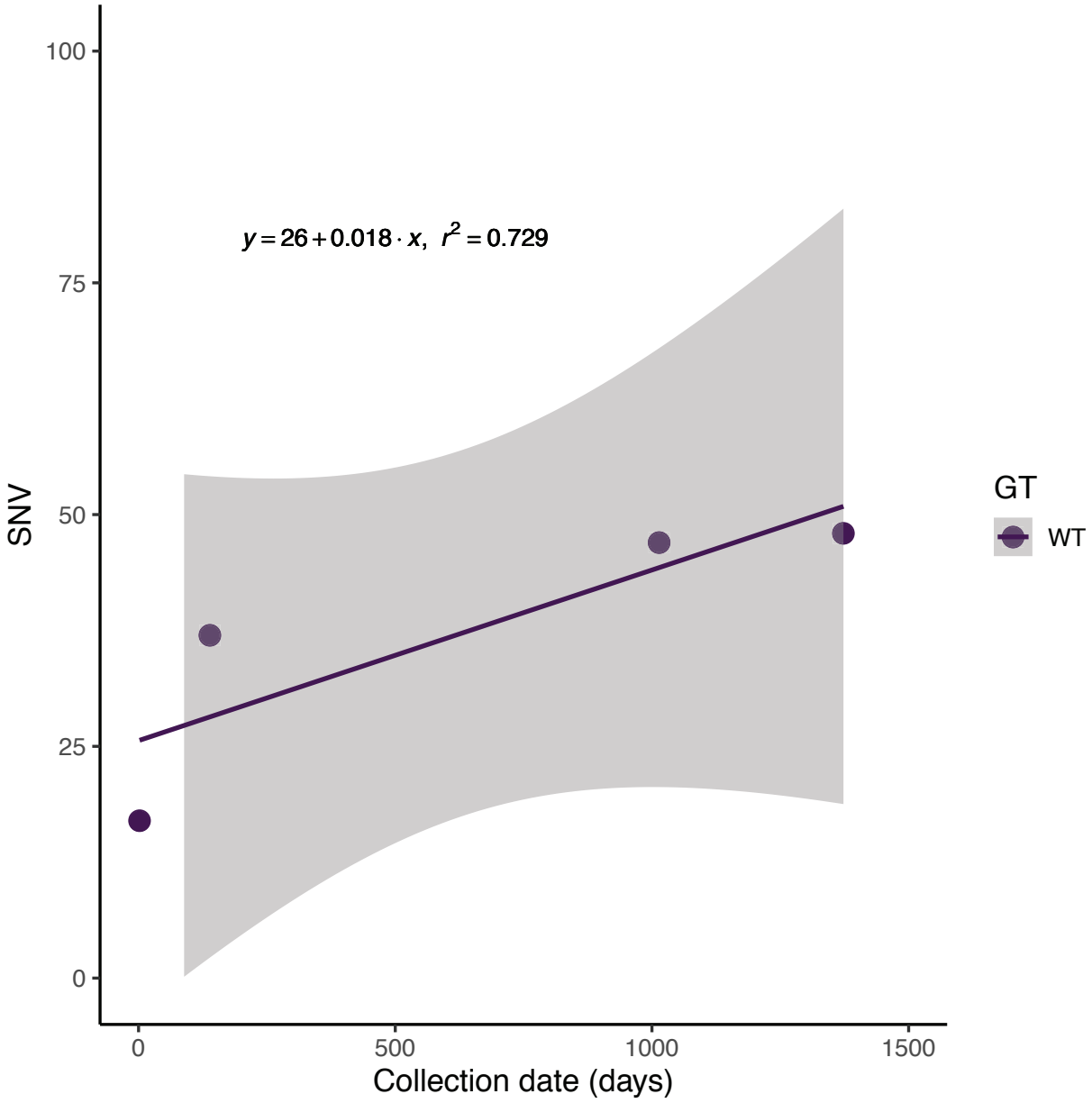


**Supplementary Figure 6. Divergence of patient isolates with wild type DnaQ gene from LCA versus collection date.** Also shown is a linear regression fit (+/- 95% CI).

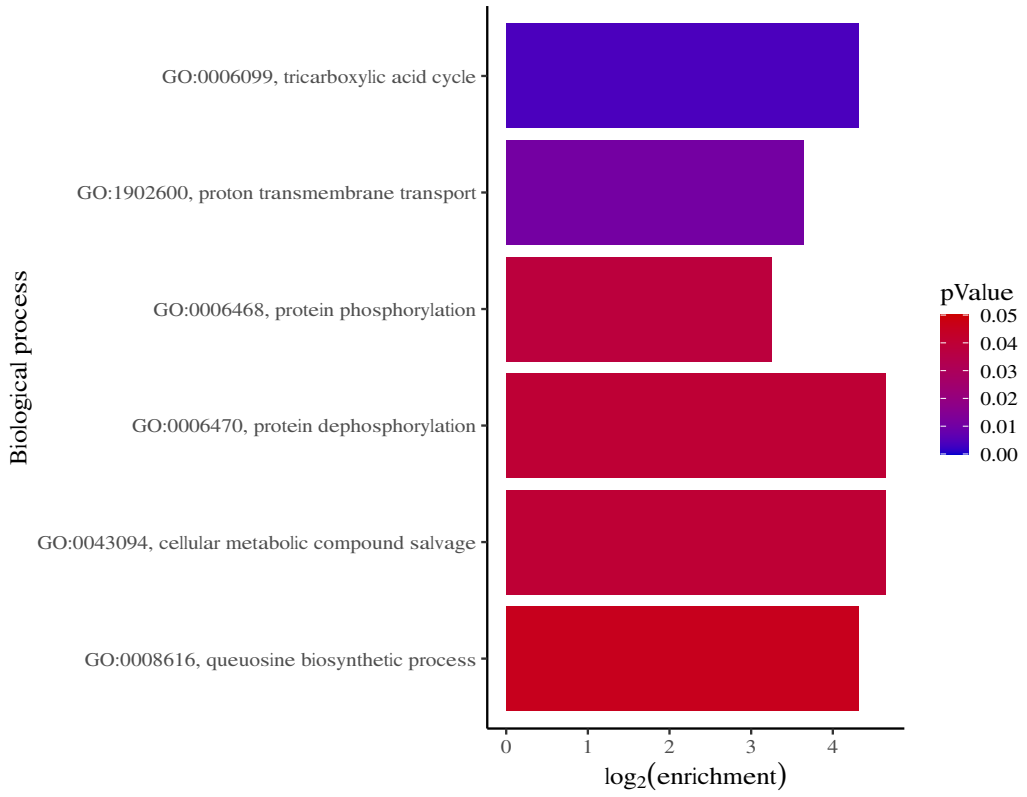


**Supplementary Figure 7. Gene ontology classification of the 25 variant targets that are shared by all DnaQ E9G proof-reading deficient isolates.** TopGO weighted GO analysis of the 25 variant targets shared by all DnaQ E9G isolates with $p<0.05$ (one-tailed Fisher's exact test) demonstrates functional enrichment of a number of cellular processes, with strongest enrichment seen in tricarboxylic acid cycle targets.

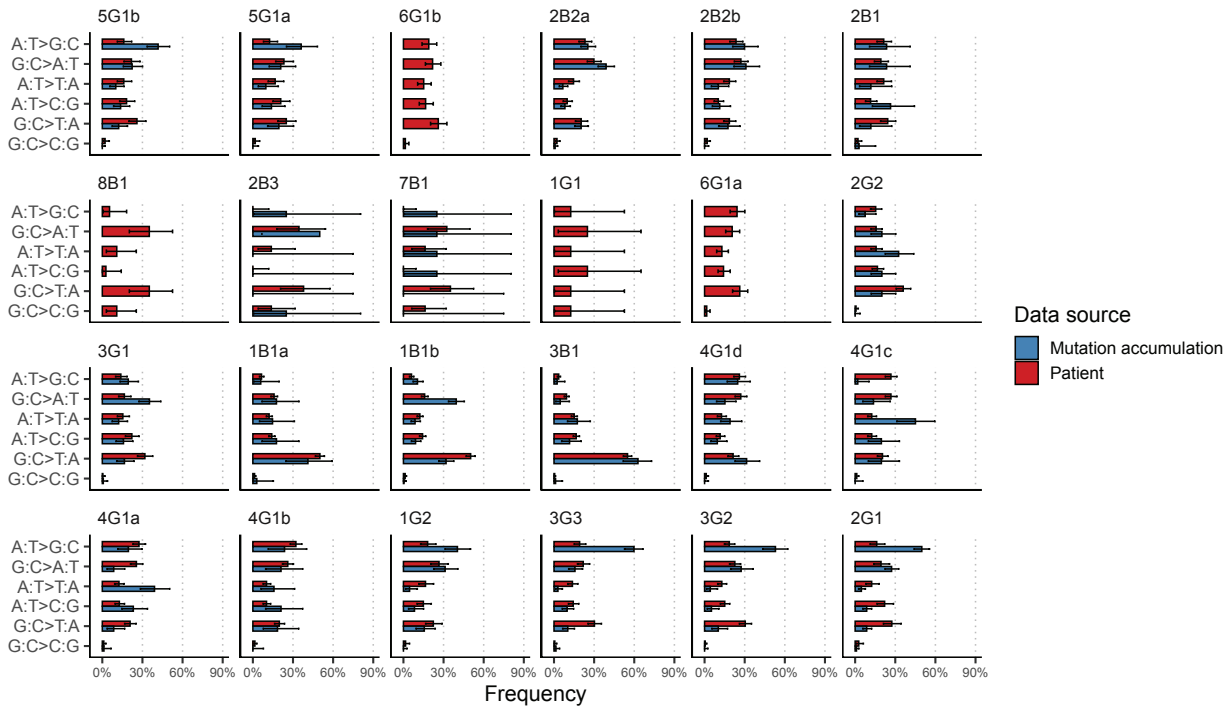


**Supplementary Figure 8. Lineage-specific mutational spectra in patient isolates largely reflects the mutational spectra observed in *in vitro* mutation accumulation experiments.** Comparison of mutational spectra present in patient isolates (red) with mutational spectra observed in *in vitro* mutation accumulation experiment, performed with the same isolates (blue). For the analysis, all data were aggregated over all set of technical replicates (see Methods for details). Bars represent the binomial estimates of frequency of each substitution type in each isolate, and the lines represent Clopper and Pearson 95$^{th}$ percentile confidence interval estimates.

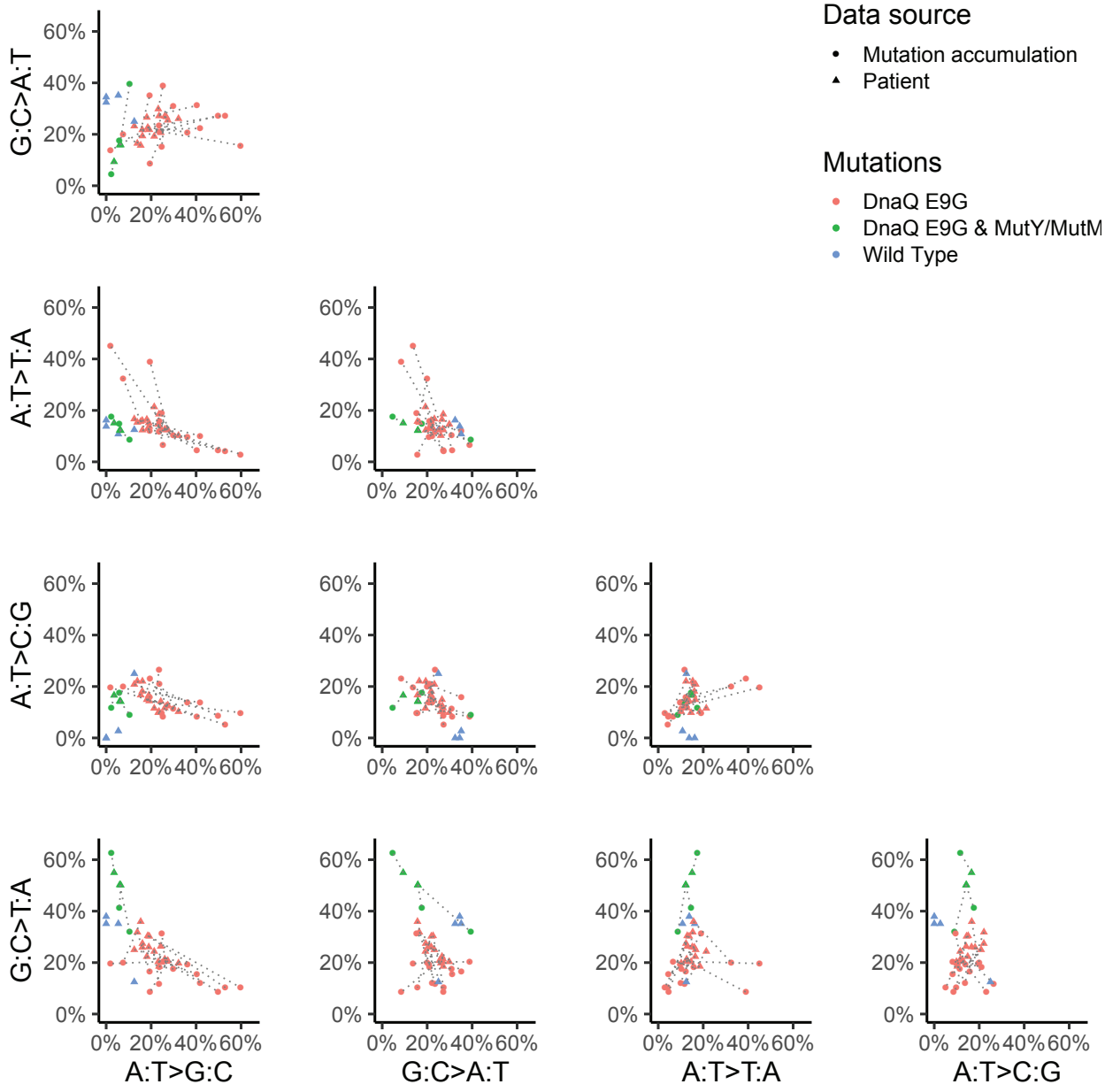


**Supplementary Figure 9. Comparison of mutational spectra in patient isolates and mutational spectra in *in vitro* mutation accumulation experiments**. Mutational spectra in patient isolates are shown as triangles, and mutational spectra observed in *in vitro* mutation accumulation experiments performed on same isolates are shown as circles, connected by a dashed line.

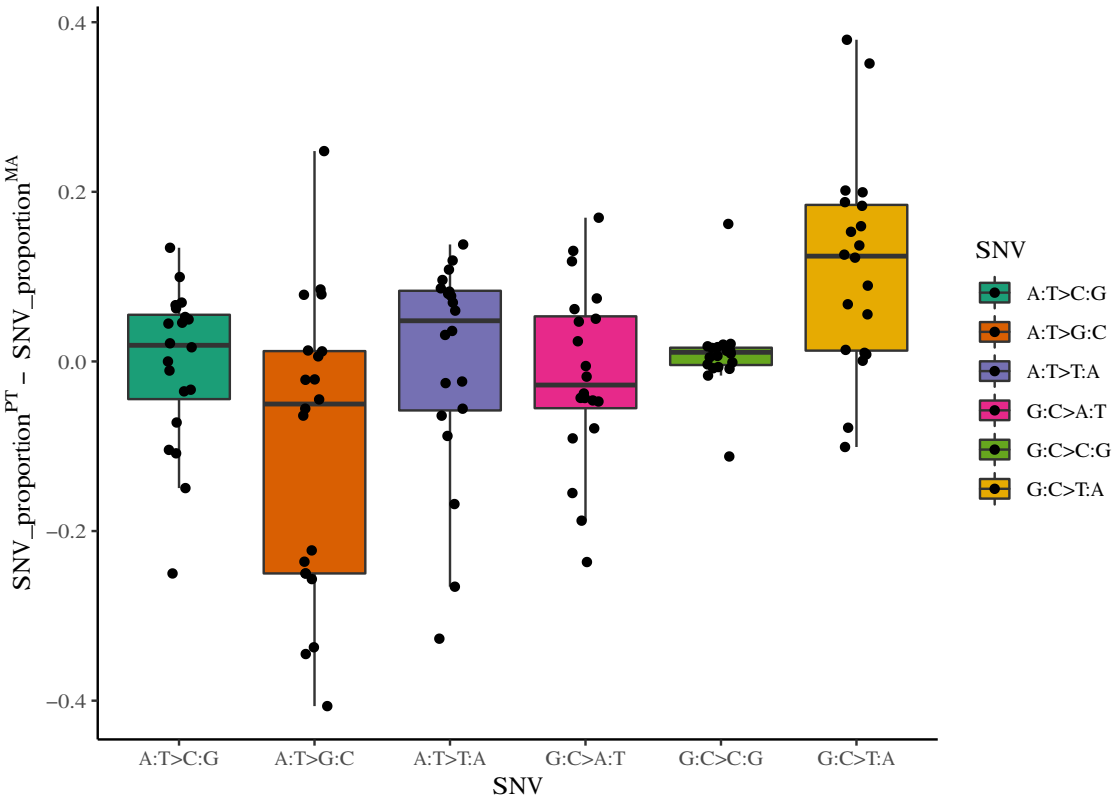


**Supplementary Figure 10. Comparison of substitution categories in patient isolates and *in vitro* mutation accumulation experiments.** Box plot shows, for each category of mutations, the difference between the substitution frequency seen in patient isolates and the frequency seen in the mutation accumulation experiment (n= 6 × 20). Horizontal lines inside boxes indicate median values, the upper and lower edges correspond to the 25th and 75th percentiles, and whiskers extend to 1.5 × IQR. The frequency of C:G>T:A substitutions is notably elevated in patient isolates, consistent with an oxidative mutagenesis signature.

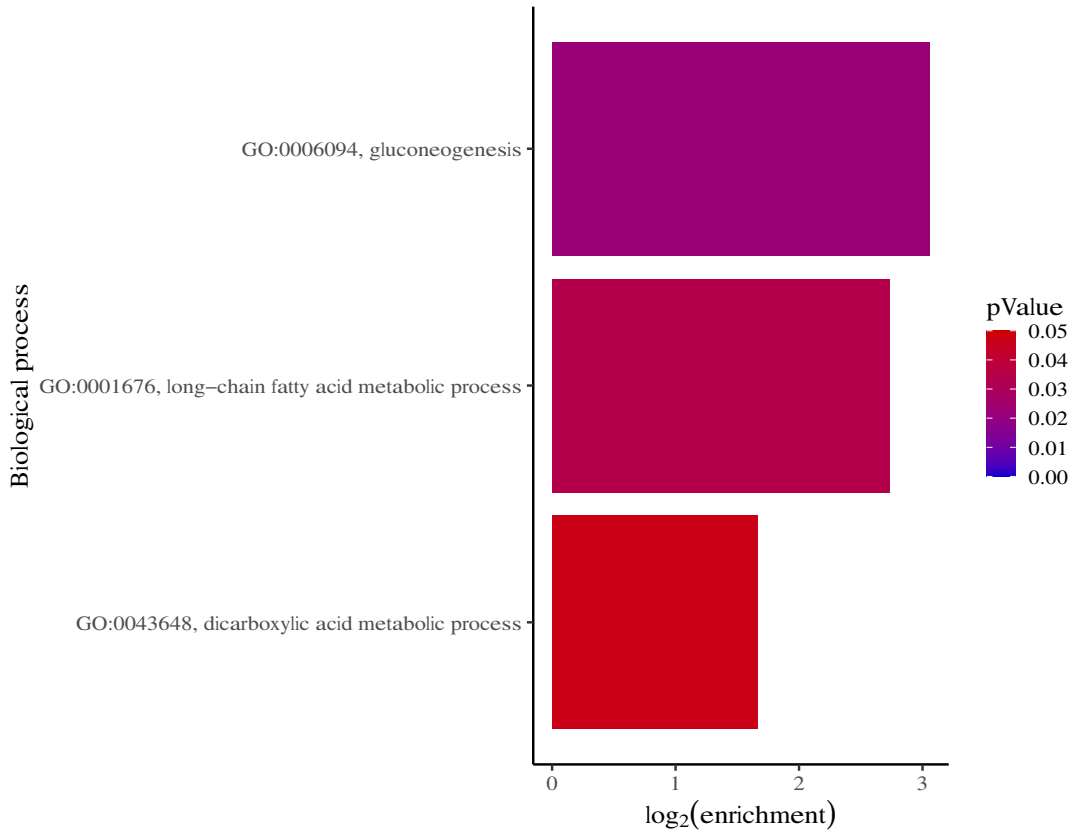


**Supplementary Figure 11. Gene ontology classification of mutational targets identified in patient isolates.** TopGO weighted analysis of targets demonstrating repeated independent mutations with $p<0.05$ (one-tailed Fisher's exact test) demonstrates enrichment of targets in gluconeogenesis, long-chain fatty acid metabolic processes and dicarboxylic acid metabolic processes.

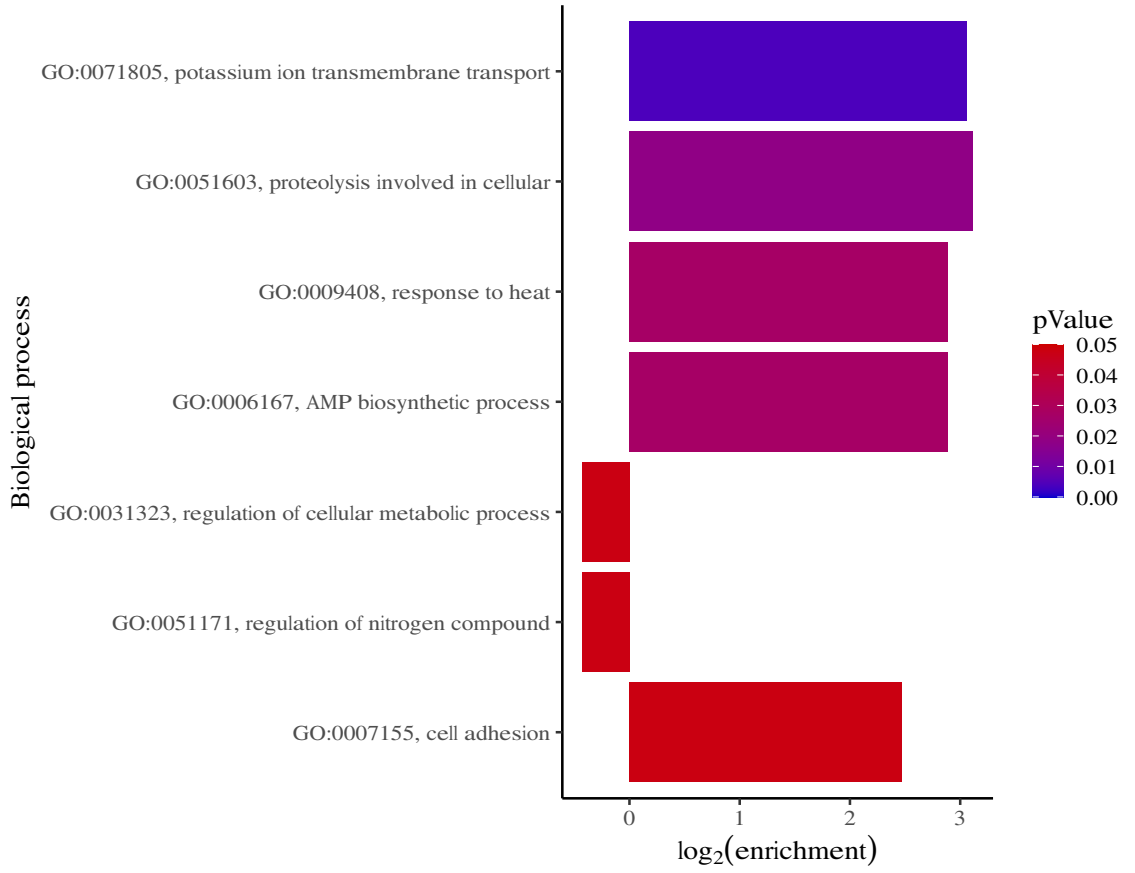


**Supplementary Figure 12. Gene ontology classification of pseudogenes identified in patient isolates.** TopGO weighted analysis of identified pseudogenes with p<0.05 (one-tailed Fisher's exact test) demonstrates functional enrichment of targets in proteolysis, response to heat, and cell adhesion.

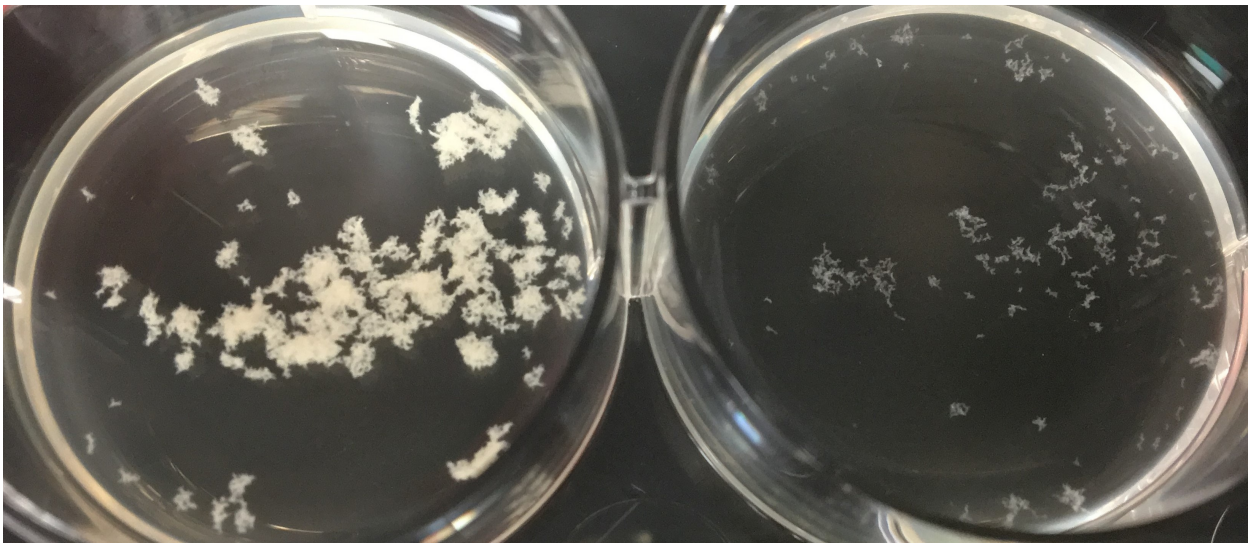

**Supplementary Figure 13. Macroscopic aggregation in liquid culture.** Cultures from the 8B1 (left) and 2B3 (right) lineages demonstrate prominent growth as macroscropic aggregates when grown in broth culture.

**Supplementary Table 1.** Colony morphologies observed for patient *B. hinzii* isolates

| Phenotype/Isolate | 1B1a | 1B1b | 1G1 | 1G2 | 2B1 | 2B2a | 2B2b | 2B3 | 2G1 | 2G2 | 3B1 | 3G1 | 3G2 | 3G3 | 4G1a | 4G1b | 4G1c | 4G1d | 5G1a | 5G1b | 8B1 |
|---|---|---|---|---|---|---|---|---|---|---|---|---|---|---|---|---|---|---|---|---|---|
| Mucoid (M) / Colonies (C) | M/C | M/C | M/C | C | M | C | M | C | C | C | M/C | C | M/C | C | C | M | C | C | C | C | C |
| Colony Size | + | ++ | ++ | +/++ | NA | +/++ | NA | +/++ | +/++ | ++ | + | ++ | + | ++ | ++ | NA | ++ | ++ | ++ | +/++ | + |
| Opaque (O) / Translucent (T) | T | O/T | O | O | O/T | O | O | O | O | O | O/T | O | O/T | O | O | O | O | O | O | O | O |

NA = Not Applicable. M/C = mixture of mucoid and single colonies. +/++ = mixture of two colony sizes. O/T = mixture of opaque and translucent.

**Supplementary Table 2.** Antimicrobial Susceptibility profiles for patient *B. hinzii* isolates

| Drug/Isolate | 1G1 | 1G2 | 2G1 | 2B1 | 2B3 | 3G2 | 3G3 |
|---|---|---|---|---|---|---|---|
| Doxycycline | 2 | 0.5 | 8 | 8 | 4 | - | - |
| Minocycline | - | - | 8 | 16 | 2 | - | - |
| Tetracycline | - | - | 8 | 32 | 4 | - | - |
| Tigecycline | - | - | 2 | 2 | 2 | 0.25 | 0.5 |
| Pip/Tazo | ≤4/4 | ≤4/4 | >128/4 | >128/4 | >128/4 | - | - |
| Azithromycin | | | - | - | - | 1 | 8 |
| Polymixin B | - | - | 1 | ≤0.25 | 2 | - | - |
| Levofloxacin | >8 | 8 | >16 | 16 | >16 | - | - |
| Trimeth/Sulfa | >8/152 | >8/152 | >8/152 | 27851 | >8/152 | - | - |
| Ceftazidime | - | - | >128 | >128 | 64 | - | - |
| Ertapenem | - | - | >8 | 4 | 4 | - | - |
| Imipenem | - | - | 4 | 2 | 2 | 1 | 1 |
| Meropenem | 8 | 8 | >8 | 4 | 4 | 4 | 8 |
| Amikacin | 4 | 4 | 32 | 16 | 8 | - | - |
| Gentamycin | 2 | 2 | 8 | 8 | 4 | - | - |
| Tobramycin | 8 | 8 | >16 | >16 | 16 | - | - |
| Cefepime | - | - | 32 | >32 | >32 | - | - |
| Colistin | - | - | 1 | ≤0.25 | 2 | <=0.25 | 4 |

Pip/Tazo = Piperacillin/Tazobactam; Trimeth/Sulfa = Trimethoprim/Sulfamethoxazole

**Supplementary Table 3.** Sequencing and assembly information for patient *B. hinzii* isolates

| Isolates | Sequencing technology | Contigs | Total length | GC (%) | Cov | N50 |
|---|---|---|---|---|---|---|
| 1G1 | PacBio | 1 | 4845358 | 66.98 | 108.28 | 4845358 |
| 1G2 | PacBio | 1 | 4898905 | 67.01 | 161.19 | 4898905 |
| 2B1 | PacBio | 1 | 4899058 | 67.01 | 161.13 | 4899058 |
| 2B3 | PacBio | 1 | 4899031 | 67.01 | 227.9 | 4899031 |
| 2G1 | PacBio | 1 | 4898869 | 67.01 | 137.45 | 4898869 |
| 1B1a | Illumina | 51 | 4874957 | 67.03 | 81.69 | 200971 |
| 1B1b | Illumina | 52 | 4875262 | 67.03 | 87.28 | 228726 |
| 1G1 | Illumina | 30 | 4819330 | 67.02 | 70.4 | 422032 |
| 1G2 | Illumina | 32 | 4873616 | 67.04 | 75.99 | 424690 |
| 2B1 | Illumina | 27 | 4874913 | 67.05 | 114.5 | 424690 |
| 2B2a | Illumina | 34 | 4872885 | 67.05 | 244.17 | 424267 |
| 2B2b | Illumina | 35 | 4872434 | 67.05 | 138.38 | 334930 |
| 2B3 | Illumina | 28 | 4874194 | 67.05 | 146.11 | 424690 |
| 2G1 | Illumina | 31 | 4874440 | 67.05 | 138.85 | 424690 |
| 2G2 | Illumina | 30 | 4874045 | 67.04 | 197.13 | 424264 |
| 3B1 | Illumina | 32 | 4870893 | 67.03 | 194.82 | 424691 |
| 3G1 | Illumina | 70 | 4867756 | 67.04 | 63.44 | 119745 |
| 3G2 | Illumina | 31 | 4874477 | 67.05 | 109.9 | 424264 |
| 3G3 | Illumina | 29 | 4873819 | 67.05 | 173.99 | 424264 |
| 4G1a | Illumina | 36 | 4873355 | 67.05 | 40.85 | 334930 |
| 4G1b | Illumina | 30 | 4874646 | 67.05 | 137.18 | 434284 |
| 4G1c | Illumina | 33 | 4874276 | 67.05 | 185.81 | 434273 |
| 4G1d | Illumina | 36 | 4874953 | 67.04 | 81.77 | 370497 |
| 5G1a | Illumina | 31 | 4874384 | 67.05 | 53.52 | 425144 |
| 5G1b | Illumina | 30 | 4873668 | 67.04 | 61.56 | 424691 |
| 6G1a | Illumina | 29 | 4874601 | 67.05 | 75.78 | 424690 |
| 6G1b | Illumina | 32 | 4874287 | 67.05 | 101.96 | 424690 |
| 7B1 | Illumina | 73 | 4867858 | 67.04 | 42.53 | 150297 |
| 8B1 | Illumina | 64 | 4829741 | 67.1 | 50.66 | 139051 |
| ATCC_51783 | Illumina | 69 | 4997723 | 65.97 | 67.09 | 118470 |
| ATCC_51784 | Illumina | 81 | 4867486 | 67.51 | 66.99 | 116274 |

**Supplementary Table 4.** Deletions in the genomes of patient isolates

| Position | Length (bp) | Gene name | Locus tag | Product | In isolates |
|---|---|---|---|---|---|
| 522746 | 267 | adoK | A_00509 | Adenosine kinase | 5G1a,5G1b,6G1b |
| 1044661 | 117 | NA | A_00961 | hypothetical protein | 1G2 |
| 1479787 | 180 | ltaE to A_01369 | A_01368 to A_01369 | 2 genes | 4G1a,4G1b,4G1c,4G1d |
| 2144786 | 53478 | gabR_2 to hsrA_2 | A_02003 to A_02051 | 49 genes | 1G1 |
| 3072620 | 1530 | NA | A_02898 | hypothetical protein | 3B1 |
| 3152552 | 455 | A_02961 | A_02961 | hypothetical protein | 3B1 |
| 3823276 | 38482 | NA | A_03624 to A_03675 | 52 genes | 8B1,8B2 |
| 4566359 | 428 | trkH | A_04354 | Trk system potassium uptake protein TrkH | 1B1a,1B1b |
| 4573054 | 333 | rsmB_2 | A_04359 | Ribosomal RNA small subunit methyltransferase B | 5G1a,5G1b,6G1b |
| 4722262 | 285 | steT | A_04511 | Serine/threonine exchanger SteT | 3B1 |

**Supplementary Table 5.** Mutational spectra from patient isolates and mutation accumulation experiments.

| Patient Isolate SNVs | 5G1b | 5G1a | 6G1b | 2B2a | 2B2b | 2B1 | 8B1 | 2B3 | 7B1 | 1G1 | 6G1a | 2G2 | 3G1 | 1B1a | 1B1b | 3B1 | 4G1d | 4G1c | 4G1a | 4G1b | 1G2 | 3G3 | 3G2 | 2G1 |
|---|---|---|---|---|---|---|---|---|---|---|---|---|---|---|---|---|---|---|---|---|---|---|---|---|
| A:T>G:C | 31 | 21 | 40 | 73 | 71 | 50 | 2 | 0 | 0 | 1 | 60 | 47 | 37 | 56 | 51 | 35 | 105 | 110 | 99 | 148 | 34 | 64 | 76 | 30 |
| G:C>A:T | 42 | 39 | 46 | 94 | 82 | 45 | 13 | 10 | 12 | 2 | 51 | 48 | 44 | 137 | 134 | 93 | 109 | 110 | 92 | 120 | 50 | 73 | 93 | 36 |
| A:T>T:A | 31 | 28 | 32 | 46 | 56 | 50 | 4 | 4 | 6 | 1 | 32 | 48 | 41 | 105 | 104 | 150 | 51 | 51 | 45 | 47 | 31 | 46 | 53 | 23 |
| A:T>C:G | 35 | 35 | 35 | 31 | 31 | 27 | 1 | 0 | 0 | 2 | 35 | 51 | 59 | 122 | 121 | 165 | 47 | 51 | 46 | 47 | 28 | 48 | 62 | 41 |
| G:C>T:A | 50 | 42 | 55 | 64 | 56 | 57 | 13 | 11 | 13 | 1 | 65 | 110 | 85 | 433 | 425 | 547 | 86 | 84 | 75 | 91 | 42 | 101 | 125 | 51 |
| G:C>C:G | 4 | 3 | 3 | 7 | 6 | 5 | 4 | 4 | 6 | 1 | 4 | 2 | 1 | 11 | 11 | 5 | 5 | 5 | 4 | 7 | 3 | 2 | 2 | 5 |

| Mutational Accumulation | 5G1b | 5G1a | 6G1b | 2B2a | 2B2b | 2B1 | 8B1 | 2B3 | 7B1 | 1G1 | 6G1a | 2G2 | 3G1 | 1B1a | 1B1b | 3B1 | 4G1d | 4G1c | 4G1a | 4G1b | 1G2 | 3G3 | 3G2 | 2G1 |
|---|---|---|---|---|---|---|---|---|---|---|---|---|---|---|---|---|---|---|---|---|---|---|---|---|
| A:T>G:C | 58 | 26 | | 65 | 29 | 8 | | 1 | 1 | | | 6 | 27 | 2 | 29 | 2 | 26 | 1 | 16 | 9 | 44 | 122 | 62 | 150 |
| G:C>A:T | 31 | 15 | | 100 | 30 | 8 | | 2 | 1 | | | 16 | 49 | 6 | 109 | 4 | 16 | 7 | 7 | 8 | 34 | 32 | 32 | 82 |
| A:T>T:A | 14 | 7 | | 17 | 10 | 4 | | 0 | 1 | | | 26 | 17 | 5 | 24 | 15 | 20 | 23 | 32 | 6 | 5 | 6 | 5 | 14 |
| A:T>C:G | 19 | 10 | | 21 | 11 | 9 | | 0 | 1 | | | 16 | 22 | 6 | 25 | 10 | 10 | 10 | 19 | 8 | 9 | 20 | 6 | 26 |
| G:C>T:A | 17 | 14 | | 52 | 17 | 4 | | 0 | 0 | | | 16 | 23 | 14 | 88 | 54 | 33 | 10 | 7 | 7 | 17 | 21 | 12 | 26 |
| G:C>C:G | 0 | 0 | | 2 | 0 | 1 | | 1 | 0 | | | 0 | 1 | 1 | 1 | 1 | 0 | 0 | 1 | 0 | 0 | 3 | 0 | 3 |

Numbers of variants in for each category of substitutions are given.

**Supplementary Table 6.** Calculation of number of passages that would be required to produce the observed number of mutations in each isolate based on *in vitro* mutation rates

| Isolate | SNVs | SNV per_division | Divisions | 95th CI divisions | Passages |
|---|---|---|---|---|---|
| 1B1a | 142 | 0.3125 | 454.4 | 325.4-655.9 | 16.7 |
| 1B1b | 132 | 2.5368 | 52 | 46.3-58.7 | 1.9 |
| 2B2a | 126 | 1.3498 | 93.3 | 82.7-105.8 | 3.4 |
| 2B2b | 117 | 0.5944 | 196.8 | 161.5-242.6 | 7.2 |
| 4G1a | 19 | 0.0773 | 245.8 | 198-309 | 9 |
| 4G1b | 317 | 0.0437 | 7261 | 5290.5-10259.9 | 266.9 |
| 4G1c | 18 | 0.0647 | 278.4 | 211.8-373.9 | 10.2 |
| 4G1d | 10 | 0.2145 | 46.6 | 38.5-57 | 1.7 |
| 5G1a | 58 | 0.3782 | 153.4 | 121.9-195.9 | 5.6 |
| 5G1b | 90 | 0.73 | 123.3 | 104.5-146.6 | 4.5 |

**Supplementary Table 7.** Additional genomes used in this study

| Strain | Accession | Genome size | Host | Country | Collection |
|---|---|---|---|---|---|
| F582 | CP012076 | 4912977 | H. sapiens | USA: WA | 1994 |
| FDAARGOS_621 | CP044059 | 4860452 | H. sapiens | USA: MI | NA |
| H568 | CP012077 | 4859884 | H. sapiens | USA: AR | 2010 |
| H720 | CP024172 | 4859886 | NA | USA: MN | 2010 |
| NCTC13199 | LR134382 | 5033537 | Chicken | Australia | 1900/1993 |
| 14-3425 | CP021398 | 4885078 | Turkey | USA: NC | 2019 |
| 243-2 | CP021400 | 4811419 | Turkey | USA: MN | 1997 |
| NCTC13200 | LT906461 | 4913806 | NA | NA | 1900/2007 |
| SV2 | CP021395 | 4809490 | Turkey | USA: VA | 2006 |
| 4134 | CP021396 | 5042960 | Turkey | USA: MN | NA |
| 4449 | CP021397 | 4898820 | Turkey | USA: MN | NA |
| TR-1212 | CP021399 | 4930681 | Turkey | USA | NA |